OXFORD

Cerebral Cortex, 2015, 1–9

doi: 10.1093/cercor/bhv031
Original Article

ORIGINAL ARTICLE

Age-Dependent Long-Term Potentiation Deficits in the Prefrontal Cortex of the *Fmr1* Knockout Mouse Model of Fragile X Syndrome

Henry G. S. Martin[1,2,3], Olivier Lassalle[1,2,3], Jonathan T. Brown[4], and Olivier J. Manzoni[1,2,3]

[1]INSERM U901, Marseille 13009, France, [2]INMED, Marseille 13009, France, [3]Université de Aix-Marseille, UMR S901, Marseille, France, and [4]Institute of Biomedical and Clinical Sciences, University of Exeter Medical School, University of Exeter, Exeter, UK

Address correspondence to Olivier Manzoni, INSERM U901, INMED, Marseille 13009, France. Email: olivier.manzoni@inserm.fr

Abstract

The most common inherited monogenetic cause of intellectual disability is Fragile X syndrome (FXS). The clinical symptoms of FXS evolve with age during adulthood; however, neurophysiological data exploring this phenomenon are limited. The *Fmr1* knockout (*Fmr1* KO) mouse models FXS, but studies in these mice of prefrontal cortex (PFC) function are underrepresented, and aging linked data are absent. We studied synaptic physiology and activity-dependent synaptic plasticity in the medial PFC of *Fmr1* KO mice from 2 to 12 months. In young adult *Fmr1* KO mice, NMDA receptor (NMDAR)-mediated long-term potentiation (LTP) is intact; however, in 12-month-old mice this LTP is impaired. In parallel, there was an increase in the AMPAR/NMDAR ratio and a concomitant decrease of synaptic NMDAR currents in 12-month-old *Fmr1* KO mice. We found that acute pharmacological blockade of $mGlu_5$ receptor in 12-month-old *Fmr1* KO mice restored a normal AMPAR/NMDAR ratio and LTP. Taken together, the data reveal an age-dependent deficit in LTP in *Fmr1* KO mice, which may correlate to some of the complex age-related deficits in FXS.

Key words: Fragile X, LTP, mGlu receptor, NMDA receptor, synaptic plasticity

Introduction

Fragile X syndrome (FXS) is a major form of inherited intellectual disability (ID) caused by the transcriptional silencing of the gene *FMR1*. The disorder is characterized by a series of physical, cognitive, and emotional symptoms that include social deficits and a diminished ability to learn. Frequently found comorbid with other complex neurological disorders, including attention deficit hyperactivity disorder, epilepsy, and anxiety (Bailey et al. 2008), FXS is also the principal monogenetic cause of autism spectrum disorders.

The *FMR1* gene product, fragile X mental retardation protein (FMRP), is an mRNA-binding protein, which is absent in the FXS brain throughout development. Principally, FMRP is found in neuronal spines where it functions as a translational repressor of a subpopulation of mRNAs linked to synaptic function. Upon suitable synaptic stimulation, FMRP is released and local mRNA translation proceeds. In the hippocampus, $mGlu_5$ receptor (mGluR5) activation engages an important synaptic signal transduction pathway leading to local translation (Ronesi and Huber 2008). Loss of FMRP results in dysregulation of this pathway and is the basis of the mGluR theory of FXS (Bear et al. 2004). This is supported by the observation that, in a mouse model of FXS, mGluR5 antagonists not only restore many of the associated changes in the synaptic structure, development, and regulation, but also some of the behavioral deficits (Dölen et al. 2007;

Michalon et al. 2012). mGluR5 antagonists have been a major focus for the development of therapeutics to treat some of the symptoms associated with FXS (Krueger and Bear 2011).

Prefrontal cortex (PFC) malfunctions are a common denominator in several neuropsychiatric diseases (Goto et al. 2010; Huntley and Howard 2010). Loss of executive function and inhibitory control are particularly prominent in the ID associated with FXS, and there is evidence of increasing ID with age (Lachiewicz et al. 1987; Wright-Talamante et al. 1996; Cornish et al. 2001; Utari et al. 2010; Schneider et al. 2013). The exact contribution of FMRP in PFC functions and in particular the synaptic basis of the age-dependent defects reported in FXS remains obscure. In the *Fmr1* knockout (*Fmr1* KO) mouse model of FXS, there is evidence of changes in PFC-mediated behaviors in young adult animals (Dölen et al. 2007; Gantois et al. 2013; Kramvis et al. 2013; Sidorov et al. 2014), and biochemical analysis of PFC synapses suggests alterations in glutamate receptors and accessory proteins in excitatory synapses (Krueger et al. 2011). During juvenile development, a hyperconnected state exists between layer V pyramidal neurons, similar to that found in other models of autism (Rinaldi et al. 2008; Testa-Silva et al. 2012). However, the increased connectivity between layer V neurons is normalized as *Fmr1* KO mice reach adolescence. In early adulthood, it has been reported that both spike-timing-dependent and D1 receptor-mediated long-term potentiation (LTP) are modified in superficial layers of the *Fmr1* KO PFC (Zhao et al. 2005; Meredith et al. 2007; Wang et al. 2008), but whether this is indicative of a general PFC dysfunction is unclear. There is evidence from the piriform cortex that an age-linked phenotype may be present in the *Fmr1* KO model. In early adulthood, *Fmr1* KO mice express stimulus-evoked LTP; however, an increasing loss in LTP is found as mice reach middle age and after (Larson et al. 2005). Whether a similar phenotype is present in the PFC and other brain regions associated with the cognitive decline found in FXS remains unexamined.

Here, we evaluated LTP in pyramidal neurons from deep layers (layer 5) of the medial PFC (mPFC) neurons in adult *Fmr1* KO mice, in both early and late adulthood. We report that LTP and NMDA receptor (NMDAR) function is impaired in the PFC of 12-month-old mice, but normal at a younger age. This age-specific reduction of synaptic plasticity may underlie part of the multiple cognitive and behavioral deficits described in aging FXS patients. Furthermore, specific inhibition of mGluR5 restored a normal AMPAR/NMDAR ratio and rescued LTP in 12-month-old *Fmr1* KO mice, extending the mGluR theory of FXS.

Materials and Methods

All mice were group-housed with 12 h light/dark cycles in compliance with the European Communities Council Directive (2010/63/EU) for the Care and Use of Laboratory Animals. Male *Fmr1* KO2 mice, null for protein, and mRNA on a C57Bl6/J genetic background were used, with wild-type (WT) littermates as a control group. Young adult mice (2 months) were 9–12 weeks and mature adult (12 months) were 12 ± 2 months of age.

Slice Preparation

Mice were anesthetized with isoflurane and decapitated according to institutional regulations. The brain was sliced (300 µm) in the coronal plane with a vibratome (Integraslice, Campden Instruments, Loughborough, UK) in a sucrose-based solution at 4 °C (in mM: 87 NaCl, 75 sucrose, 25 glucose, 5 KCl, 21 $MgCl_2$, 0.5 $CaCl_2$, and 1.25 NaH_2PO_4). Slices were allowed to recover for 60 min at 32–35 °C in artificial cerebrospinal fluid (aCSF) containing 126 mM NaCl, 2.5 mM KCl, 2.4 mM $MgCl_2$, 1.2 mM $CaCl_2$, 18 mM $NaHCO_3$, 1.2 mM NaH_2PO_4, and 11 mM glucose, equilibrated with 95% O_2/5% CO_2. Slices were then maintained at 22 ± 2 °C until recording.

Electrophysiology

Whole-cell patch-clamp and extracellular field recordings were made from layer 5 pyramidal cells in the prelimbic cortex (Lafourcade et al. 2007). For recording, slices were superfused (2 mL/min) with aCSF. All experiments were done at 32–35 °C. The recording aCSF contained picrotoxin (100 µM) to block $GABA_A$ receptors. To evoke synaptic currents, 100–200 µs stimuli were delivered at 0.1 Hz through an ACSF-filled glass electrode positioned dorsal to the recording electrode in layer V. For extracellular field experiments, the recording pipette was filled with aCSF. The glutamatergic nature of the field excitatory postsynaptic potential (fEPSP) was confirmed at the end of the experiments using the ionotropic glutamate receptor antagonist 6-cyano-7-nitroquinoxaline-2,3-dione (CNQX, 20 µM) that specifically blocked the synaptic component without altering the non-synaptic component. LTP was induced by a theta burst protocol as previously described (Iafrati et al. 2014).

For whole-cell patch-clamp, pyramidal neurons in PFC layer 5 were visualized using an infrared microscope (BX-50, Olympus). Experiments were made with electrodes containing 143 mM cesium methanesulfonate (CH_3O_3SCs, voltage clamp) or 145 mM potassium gluconate (KGlu, current clamp and voltage clamp), with 5 mM NaCl, 1 mM $MgCl_2$, 1 mM EGTA, 0.3 mM $CaCl_2$, 2 mM Na^{2+}-ATP, 0.3 mM Na^{+}-GTP, 10 mM glucose buffered with 10 mM HEPES, pH 7.3, osmolarity 290 mOsm. Electrode resistance was 3–5 MΩ. If access resistance was >20 MΩ or changed by >20%, the experiment was rejected. Junction potentials were not correct. To perform current–voltage (*I*–*V*) curves and to test neuronal excitability, a series of hyperpolarizing and depolarizing current steps were applied immediately after breaking in the cell.

Spontaneous AMPAR- and NMDAR-mediated excitatory postsynaptic currents (EPSC) were recorded in the voltage-clamp configuration at −70 or +40 mV in the presence of 2,3-dihydroxy-6-nitro-7-sulfamoyl-benzo[f]quinoxaline-2,3-dione to block AMPAR-mediated events (NBQX, 10 µM).

Data Acquisition and Analysis

Data were recorded on a MultiClamp700B (Axon Instruments), filtered at 2 or 10 kHz (spike characterization), digitized (10 or 50 kHz, DigiData 1440A, Axon Instrument), collected using Clampex 10.2, and analyzed using Clampfit 10.2 (all from Molecular Device, Sunnyvale, CA, USA). AMPAR/NMDAR ratios were calculated from monosynaptic EPSCs by dividing the averaged EPSC (30 events) amplitude recorded at −70 mV, by the averaged EPSC (30 events) current 30 ms after the peak AMPAR-mediated event at +40 mV, a time point where rapidly gated AMPAR currents are negligible. Analysis of both area and amplitude of fEPSPs and EPSCs was performed (graphs depict amplitudes for patch-clamp experiments and areas for field recordings). The magnitude of LTP was calculated 35–40 min after theta burst stimulation (TBS) as a percentage of baseline responses. LTP data were collated and analyzed from throughout the lifetime of the project, except during experimental treatments where a subset of interleaved control experiments was analyzed. Spontaneous NMDAR- and AMPAR-mediated EPSCs were analyzed with Axograph X (Axograph). Spontaneous events were identified by passing a variable amplitude prototypical AMPAR (τ_{rise} = 0.5 ms, τ_{decay} = 3 ms; 10 ms window; noise threshold: −3) or NMDAR

(τ_{rise} = 3 ms, τ_{decay} = 50 ms; 50 ms window; noise threshold: +5) event over the recording as previously described (Iafrati et al. 2014). Overlapping events were ignored. Tau-weighted (τ_w) was calculated from a double exponential fit of the NBQX-isolated NMDAR currents at +40 mV with the formula: $\tau_w = (\tau_1 * a_1) + (\tau_2 * a_2)$, where a_1 and a_2 are the relative amplitudes of the 2 exponential components. Intrinsic properties were quantified in MATLAB (MathWorks) using custom routines. Sag values were calculated from a hyperpolarizing current clamp step leading to a minimum membrane potential of at least −100 mV (typically −400 pA) and were expressed as a percent of the total change in membrane potential. Statistical analysis of data was performed with GraphPad Prism (GraphPad Software, Inc., La Jolla, CA, USA) using tests indicated in the main text after outlier subtraction.

All values are given as mean ± standard error, statistical significance was set at $^*P < 0.05$ and $^{**}P < 0.01$, and n values correspond to individual animals.

Drugs

Drugs were added at the final concentration to the recording aCSF media from DMSO (Picrotoxin and CNQX) or water [2-Methyl-6-(phenylethynyl)pyridine (MPEP) and NBQX] stocks. Picrotoxin was from Sigma (St. Quentin Fallavier, France), and MPEP, CNQX, and NBQX were from the National Institutes of Mental Health's Chemical Synthesis and Drug Supply Program (Rockville, MD, USA).

Results

Theta Burst-Induced LTP Is Selectively Impaired in the PFC of 12-Month-Old *Fmr1* KO Mice

In the mouse mPFC, moderate TBS induces a robust NMDAR-mediated LTP of deep layer pyramidal excitatory synapses throughout life (Iafrati et al. 2014). Previous reports suggest that late onset deficits in LTP may be present in a subset of cortical structures in *Fmr1* KO mice (Larson et al. 2005; Gocel and Larson 2012); however, whether a similar late onset deficit in LTP is present in the mPFC is unknown. We asked if a parallel deficit in LTP might be present in the *Fmr1* KO mouse. Taking a cross-sectional approach, we challenged mPFC brain slices with a short TBS protocol at 2 and 12 months. As expected, TBS induced a robust LTP in WT mice in young adulthood, and in contrast to reported deficits in layer II/III PFC LTP (Zhao et al. 2005; Meredith et al. 2007), we were also able to induce LTP in *Fmr1* KO littermates (Fig. 1*A*). The cumulative distribution plot of individual experiments from both groups showed a similar potentiation in fEPSP post TBS (Fig. 1*B*; $P = 0.136$, Kolmogorov–Smirnov test); furthermore, the mean percent LTP was the same in both groups (Fig. 1*C*; percent LTP: WT 23.97 ± 7.20%; 12-month-old *Fmr1* KO 21.20 ± 4.95%; $P = 0.874$, Mann–Whitney *U* test). In line with the idea that the PFC remains plastic throughout normal aging, in 12-month-old WT mice TBS induced an increase in fEPSPs identical to younger animals. However, when we challenged 12-month-old *Fmr1* KO animals with TBS-LTP, we observed a significant impairment (Fig. 1*D*). Although post-tetanus potentiation was observed in both genotypes (compare the first 3 min post TBS, Fig. 1*D*), the potentiation of the fEPSP was much reduced in 12-month-old *Fmr1* KO animals for the duration of the recording. Cumulative probability distribution plots of the normalized individual experiments further showed that the potentiation in fEPSPs was left-shifted and smaller in 12-month-old *Fmr1* KO mice (Fig. 1*E*; $P = 0.003$, Kolmogorov–Smirnov test). Furthermore, the mean percent LTP (Fig. 1*F*) was reduced by approximately 50% (percent LTP: WT 20.81 ± 3.96%; 12-month-old *Fmr1* KO 10.88 ± 2.69%; $P = 0.024$, Mann–Whitney *U* test). These data reveal that the ability to express LTP is impaired in

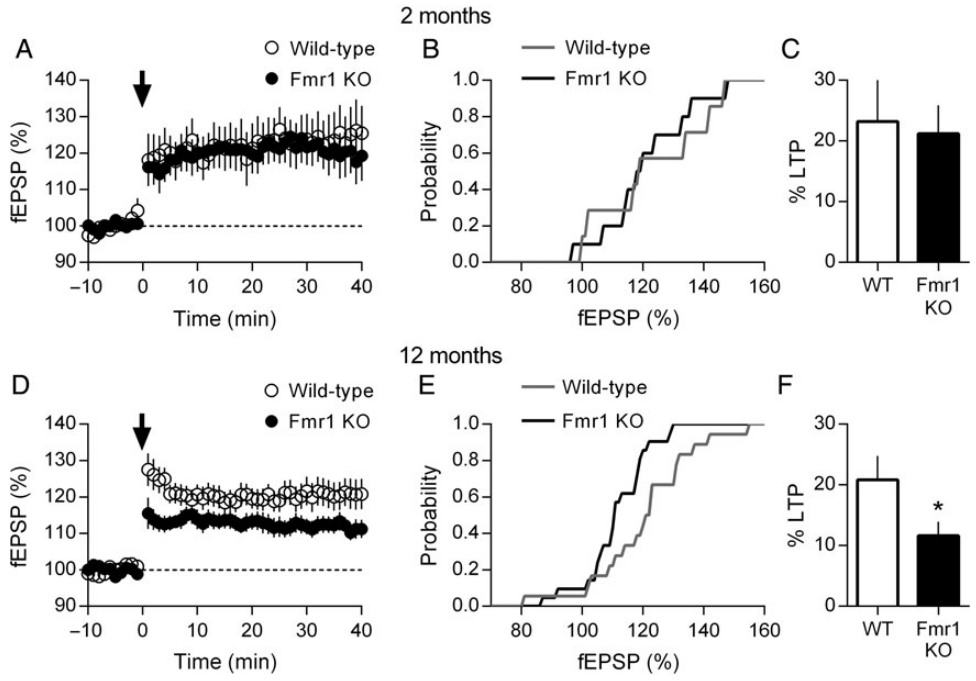

Figure 1. Age-specific impairment of LTP in the PFC of 12-month-old *Fmr1* KO. (*A*) TBS (indicated by arrow) induction of LTP in young adult mice (2 months) from mPFC layer 5 in WT mice and *Fmr1* KO littermates (WT, $n = 7$; *Fmr1* KO, $n = 10$). (*B*) Cumulative probability distribution of percent change from baseline in fEPSP 35–40 min post TBS from individual experiments. (*C*) Mean percent LTP in WT and *Fmr1* KO young adult mice. (*D*) Identical TBS-LTP induction protocol but recording from 12-month-old animals (WT, $n = 19$; *Fmr1* KO, $n = 25$). (*E*) Cumulative probability distribution of percent change in fEPSP from individual experiments. (*F*) Summary bar chart of percent LTP from 12-month-old animals ($^*P < 0.05$).

12-month-old *Fmr1* KO mice, but unaffected in young adult *Fmr1* KO mice.

Age-Specific Augmentation of the AMPAR/NMDAR Ratio in 12-Month-Old PFC Neurons

In the valproate rat model of autism, LTP and the relative synaptic weight of AMPAR to NMDAR covariate in an age-dependent manner (Rinaldi et al. 2007; Walcott et al. 2011; Martin and Manzoni 2014). We recently reported that the reduction of LTP in adult, but not juvenile valproate-treated, rats was accompanied by a large increase in the ratio between AMPAR current and NMDAR synaptic current, the AMPAR/NMDAR ratio (Martin and Manzoni 2014). Consequently, we searched for changes in the relative weight of AMPAR and NMDAR at mPFC synapses in young and 12-month-old *Fmr1* KO mice.

Using AMPAR currents at −70 mV as a synaptic control, we recorded evoked NMDAR currents at +40 mV (Fig. 2A). In young adult mice, the AMPAR/NMDAR ratio was similar in both groups of animals (WT 2.44 ± 0.34, $n = 10$; *Fmr1* KO 2.32 ± 0.26, $n = 6$; $P = 0.946$, Mann–Whitney *U* test). However, in 12-month-old mice, we found a significant increase in the AMPAR/NMDAR ratio in the *Fmr1* KO compared with age-matched controls (Fig. 2B; WT 2.34 ± 0.30, $n = 12$, *Fmr1* KO 3.87 ± 0.46, $n = 12$; $P = 0.021$, Mann–Whitney *U* test). The relative magnitude of the response at +40 mV indicated a probable reduction in NMDAR currents (Fig. 2A, right). The AMPAR/NMDAR ratio in 12-month-old *Fmr1* KO mice was also increased relative to young *Fmr1* KO animals, whereas in WT mice no age-linked change in the AMPAR/NMDAR ratio was observed.

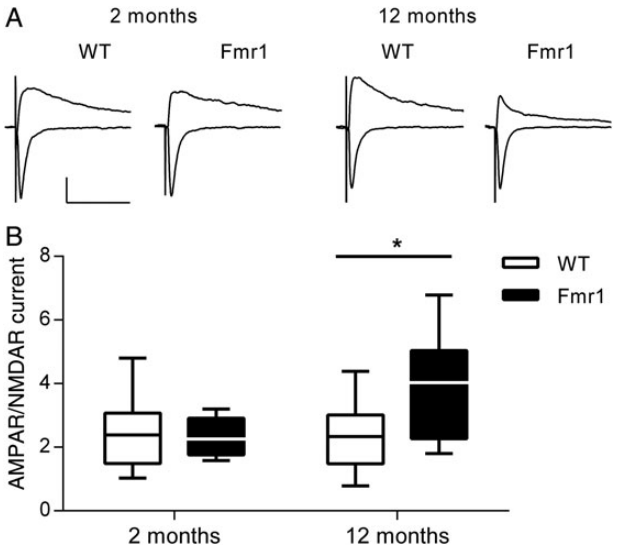

Figure 2. Age-dependent increase in the AMPAR/NMDAR ratio in layer 5 mPFC pyramidal neurons from *Fmr1* KO mice. (*A*) Example evoked EPSCs recorded from layer 5 pyramidal neurons voltage-clamped at either −70 or +40 mV from young and 12-month-old *Fmr1* KO mice with WT littermates (scale bar: 50 ms, 50 pA). (*B*) Box plot showing the interquartile range with whiskers at minimum and maximum data points of AMPAR/NMDAR ratio (*n* values: 2 months WT = 10, *Fmr1* KO = 6; 12 months: WT = 12, *Fmr1* KO = 12). Horizontal lines represent the mean AMPAR/NMDAR ratio (*$P < 0.05$).

Decreased NMDAR Synaptic Currents in 12-Month-Old *Fmr1* KO Adult PFC Neurons

We first assessed synaptic function by recording evoked fEPSP. The input/output relationship was similar in 12-month-old WT mice and *Fmr1* KO littermates, showing that the overall strength of mPFC glutamatergic synapses was unaltered (Supplementary Fig. 1). Visually identifying pyramidal neurons in layer 5, we measured spontaneous activity. Consistent with the absence of a change in input/output properties, spontaneous activity was similar in both WT and *Fmr1* KO 12-month-old mice (Fig. 3A). The mean amplitude and distribution of events of spontaneous EPSCs (sEPSC) was almost identical between *Fmr1* KO animals and WT littermates (Fig 3B; $P = 0.966$, Kolmogorov–Smirnov test). Furthermore, the mean interval between sEPSCs was unchanged between 12-month-old *Fmr1* KO and WT littermates and the distribution of events was similar, indicating that spontaneous events occur at the same frequency (Fig 3C; $P = 0.890$, Kolmogorov–Smirnov test). At resting membrane potential, sEPSCs are predominantly due to AMPAR channel openings. Therefore, to measure NMDAR-mediated spontaneous events, we recorded sEPSCs at +40 mV, while blocking AMPAR-mediated currents. Surprisingly, in contrast to AMPAR events, we found that NMDAR spontaneous events from pyramidal neurons from *Fmr1* KO animals were less frequent and of a smaller amplitude than WT littermates (Fig. 3D). Analyzing spontaneous NMDAR events by comparing their cumulative distributions, the amplitude of events in *Fmr1* KO animals was left-shifted, indicating a reduced number of large events compared with WT controls (Fig. 3E; $P = 0.002$, Kolmogorov–Smirnov test). There was also a reduction in the mean spontaneous amplitude, which was 12% lower in *Fmr1* KO slices ($P = 0.049$; Mann–Whitney *U* test). Furthermore, the recordings indicated that the relative interval between events was particularly affected in 12-month-old *Fmr1* KO animals with a strong right-shift in the cumulative plot (Fig 3F; $P < 0.001$, Kolmogorov–Smirnov test). This resulted in a highly significant increase of the interval between NMDAR-mediated events in 12-month-old *Fmr1* KO animals ($P = 0.005$, Mann–Whitney *U* test). When we recorded spontaneous NMDAR-mediated events in young adult PFC, there was no significant difference in the amplitude (WT: 41.95 ± 1.55 pA, $n = 5$; *Fmr1* KO: 38.86 ± 0.75 pA, $n = 5$; $P = 0.135$, Mann–Whitney *U* test) nor in the interevent interval (WT: 0.74 ± 0.11 s, $n = 5$; *Fmr1* KO: 0.64 ± 0.05 s, $n = 5$; $P = 0.500$, Mann–Whitney *U* test) between *Fmr1* KO and WT littermates.

Thus, in contrast to the piriform cortex, where a stable reduction in NMDAR synaptic currents is seen throughout adulthood in the *Fmr1* KO mouse (Gocel and Larson 2012), our data demonstrate that, in the PFC, the alteration of synaptic NMDAR currents is restricted to 12-month-old *Fmr1* KO mice. Furthermore, we found that the decay kinetics of NMDAR-mediated EPSCs in these 12-month-old *Fmr1* KO mice and WT littermates were similar (WT: $\tau_w = 88.20 \pm 2.97$, $n = 10$; *Fmr1* KO: $\tau_w = 96.70 \pm 2.25$, $n = 8$; $P = 0.121$ Mann–Whitney *U* test). This suggests that the reduction in LTP and the increase in the AMPAR/NMDAR ratio, rather than be due to a change in NMDAR kinetics or subunit composition, derive from a general reduction of NMDAR-mediated synaptic currents in these older animals.

Normal Intrinsic Properties of PFC Pyramidal Neurons in Aged *Fmr1* KO Mice

Given our observed age-dependent LTP deficits in the mPFC of 12-month-old *Fmr1* KO mice, we wondered if there might be wider functional consequences to deep layer principal neurons due to this aberrant activity in 12-month-old mice. In the hippocampus, pyramidal cells from *Fmr1* KO mice have increased potassium channel function (Gross et al. 2011; Lee et al. 2011;

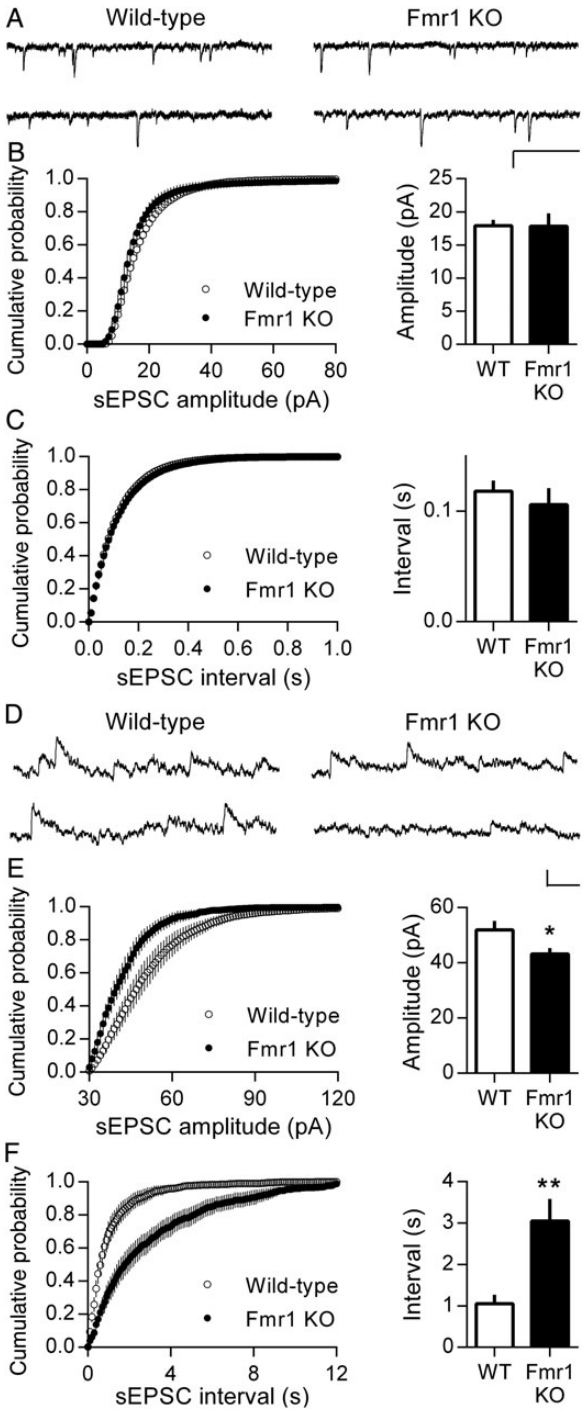

Figure 3. Reduced spontaneous NMDAR but not AMPAR-mediated events in 12-month-old *Fmr1* KO mice. (*A*) Sample traces from layer 5 mPFC pyramidal neurons clamped at −70 mV from WT and *Fmr1* KO animals (scale bar: 0.2 s, 20 pA). (*B*) Cumulative probability plot of measured sEPSC event amplitudes. Summary bar chart shows mean AMPAR event sEPSC amplitude. (*C*) Cumulative probability plot of interval between measured sEPSC events. Summary bar chart shows mean AMPAR event sEPSC interval (WT, $n = 6$; *Fmr1* KO, $n = 5$). (*D*) Sample traces of isolated spontaneous NMDAR-mediated EPSCs from mPFC neurons clamped at +40 mV from 12-month-old animals (scale bar: 0.2 s, 50 pA). (*E*) Cumulative probability plot of measured sEPSC event amplitudes. Right: summary bar chart shows mean NMDAR event sEPSC amplitude (WT, $n = 9$; *Fmr1* KO, $n = 8$). (*F*) Cumulative probability plot of interval between measured sEPSC events. Right: summary bar chart shows mean NMDAR event sEPSC interval (*$P < 0.05$, **$P < 0.01$).

Brager et al. 2012), and thus we first assessed the intrinsic properties of layer 5 mPFC neurons. Irrespective of their genotype, all recorded pyramidal neurons showed similar membrane profiles in response to a series of somatic current steps (Fig. 4A). Furthermore, the membrane capacitance (C_m: WT 113.0 ± 10.95 pF, $n = 14$; *Fmr1* KO 100.6 ± 6.463 pF, $n = 23$) and resting membrane potential (V_m: WT −71.71 ± 1.35 mV, $n = 14$; *Fmr1*$^{-/-}$ −70.45 ± 0.75 mV, $n = 22$) were unchanged between genotypes. The prominent sag in response to hyperpolarizing steps found in layer 5 pyramidal neurons was also similar in WT and *Fmr1* KO 12-month-old animals (Fig. 4B), indicative of normal I_h function. Spike profiles from individual layer 5 pyramidal neurons were induced by a standard current step injection (Fig. 4C). Spike threshold, spiking frequency, and spike adaption were comparable between the 2 groups. Thus, *Fmr1* KO in 12-month-old mice does not impact the gross intrinsic properties of PFC pyramidal.

Inhibition of mGluR5 Restores Normal LTP and AMPAR/NMDAR Ratio in 12-Month-Old *Fmr1* KO Mice

One of the most promising therapeutic routes for the treatment of FXS is the reduction in mGluR5 function (Michalon et al. 2012). This strategy was developed from the now well-described hyperactivity of the receptor and its downstream partners in the hippocampus of *Fmr1* KO animals (Ronesi and Huber 2008). In some cases, LTP impairments in *Fmr1* KO mice can be rescued by blocking group I mGluR (Xu et al. 2012; Chen et al. 2014); but see Suvrathan et al. (2010). Therefore, we wondered if reducing mGluR5 function might allow subsequent induction of LTP in the PFC of 12-month-old *Fmr1* KO. Using MPEP to block mGluR5 activity, we preincubated *Fmr1* KO mPFC slices for at least 1 h in the drug before inducing TBS-LTP. With this treatment, a recovery of LTP was apparent compared with matched control *Fmr1* KO mice (Fig 5A). Expressing the LTP as a percent change in fEPSP 35–40 min post TBS, a significant increase in LTP is present in MPEP-treated slices (Fig 5A, insert; *Fmr1* KO: 9.96 ± 3.75%, *Fmr1* KO MPEP: 20.54 ± 3.85%, $P = 0.040$, Mann–Whitney *U* test). Importantly, the LTP-induced increase in fEPSP has a magnitude similar to 12-month-old WT animals and is not significantly different from WT MPEP exposed slices (Fig. 5B). Using the same MPEP treatment regime, we also recorded AMPAR/NMDAR ratios from layer 5 pyramidal neurons from 12-month-old WT and *Fmr1* KO mice. Similar to TBS-LTP, we saw an MPEP-mediated effect on the AMPAR/NMDAR ratio (Fig. 5C). Notably, the significant increase in the AMPAR/NMDAR ratio found between WT and *Fmr1* KO was not present with MPEP treatment. Thus, by modulating mGluR5 function in 12-month-old *Fmr1* KO animals, it is possible to recover normal LTP in the PFC, most likely due to a normalization of NMDAR function.

Discussion

Here, we delineate changes in PFC synaptic plasticity in a mouse model of FXS between early and late adulthood. We found that, during early adulthood, *Fmr1* KO mice express normal LTP, but that during middle to late adulthood *Fmr1* KO mice show significantly reduced potentiation in response to LTP stimulation patterns. Thus, in the absence of FMRP, 12-month-old mice are defective for PFC LTP, while young adults are spared. Concurrent with the weakening in LTP, we found a reduction in NMDAR activity in 12-month-old *Fmr1* KO mice, demonstrated by both a relative increase in AMPAR/NMDAR ratio and a reduction in spontaneous NMDAR currents. Finally, acute treatment with

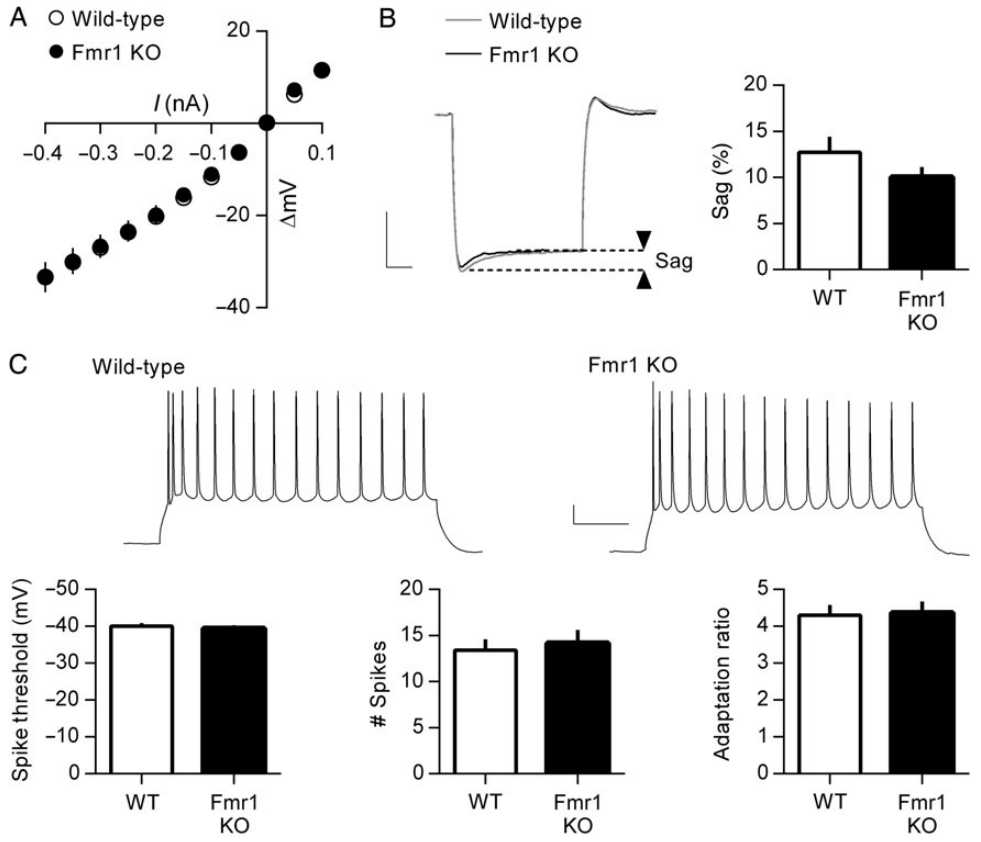

Figure 4. Intrinsic properties of layer 5 mPFC pyramidal neurons are not changed in 12-month-old *Fmr1* KO mice. (*A*) Current–voltage (*I–V*) plot from visually identified pyramidal neurons. Change in cell voltage in response to hyperpolarizing and depolarizing current steps from 12-month-old WT and *Fmr1* KO mice. (*B*) Example traces from neurons in response to hyperpolarizing current step indicating voltage sag measurement (left), bar chart of average sag voltage from WT and *Fmr1* KO animals (right). (*C*) Sample spike trains in response to 300 pA depolarizing current step from WT and KO animals (top). Quantification of neuronal spiking properties (left to right): spike threshold of first spike; number of spikes in 500 ms interval in response to 300 pA depolarizing current step; and spike adaption ratio (ratio of interval between first and last spikes; WT, $n = 14$; *Fmr1* KO, $n = 19$; scale bar: 100 ms, 10 mV).

the mGluR5 antagonist MPEP reduced the AMPAR/NMDAR in 12-month-old *Fmr1* KO mice and restored LTP.

Deficits in synaptic plasticity have been widely reported in *Fmr1* KO mice. However, the observed changes in LTP are variable, linked either to stimulation protocol or specific brain region (Sidorov et al. 2013). In contrast to our findings in layer 5 mPFC, other groups have found deficits in LTP during early adulthood in layer II/III neurons from *Fmr1* KO mice (Zhao et al. 2005; Meredith et al. 2007). This layer-specific loss in LTP appears to be linked to threshold changes in calcium signaling in the postsynaptic cell and may be restored through environmental enrichment (Meredith et al. 2007) or modulation of the dopaminergic system (Wang et al. 2008). In contrast to 12-month-old layer 5 neurons, where we found reduced NMDAR function, no changes in NMDAR-mediated currents are found in these young adult neurons (Zhao et al. 2005). Instead, the age-linked loss of LTP in 12-month-old *Fmr1* KO mice seen here appears to share greater similarities with deficits found in the dentate gyrus (DG) and piriform cortex. High-frequency stimulation elicits a robust LTP in CA1 pyramidal neurons, but not the DG in *Fmr1* KO mice (Eadie et al. 2012; Franklin et al. 2014). In common with the biochemical reduction in NMDAR and accessory proteins found in the PFC (Krueger et al. 2011), DG neurons have lower expression of NMDAR subunits and reduced NMDAR-mediated currents (Yun and Trommer 2011; Bostrom et al. 2013). Likewise, layer Ib neurons of the lateral piriform cortex show a reduction of TBS-LTP at 12 months in *Fmr1* KO mice, but not in younger animals (Larson et al. 2005). In parallel to our findings, piriform cortex neurons also show a decline in NMDAR function (Gocel and Larson 2012), correlating the reduction in LTP with the loss of NMDAR-mediated currents.

In juvenile *Fmr1* KO mice, downregulation of AMPAR-mediated responses relative to NMDAR is found in both the cortex and the hippocampus (Hu et al. 2008; Pilpel et al. 2009; Till et al. 2012), affecting both somatosensory critical period patterning and synaptic plasticity (Hu et al. 2008; Pilpel et al. 2009; Harlow et al. 2010). However, in early adulthood, cortical synaptic AMPAR and NMDAR expression and function appear to normalize in the cortex (Zhao et al. 2005; Schütt et al. 2009). In agreement, we found that PFC spontaneous NMDAR synaptic currents are similar between *Fmr1* KO and WT littermates in early adulthood. However, in 12-month-old mice, we found a significant reduction in both spontaneous NMDAR current amplitude and frequency. The reduction in spontaneous NMDAR frequency is likely due to the drop in event amplitude to below our detection threshold, since we found no evidence of reduced spontaneous AMPAR-mediated events in the same mice. This is consistent with our observed increase in the AMPAR/NMDAR ratio and measurement of NMDAR EPSC decay kinetics suggesting that the changes found in the 12-month-old *Fmr1* KO PFC are due to a general reduction in synaptic NMDARs.

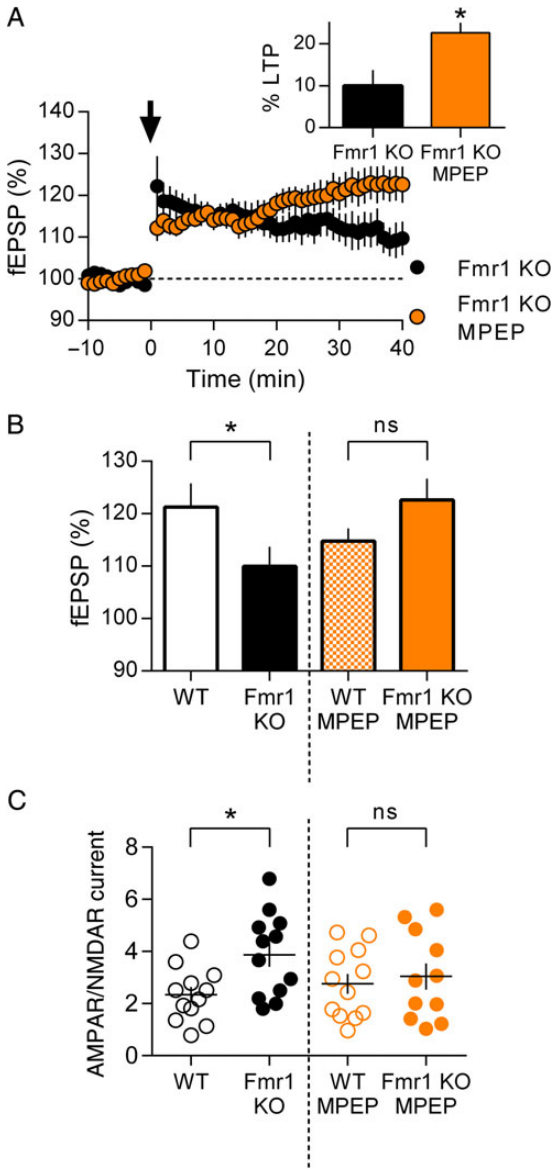

Figure 5. Acute pharmacological blockade of mGluR5 restores LTP and AMPAR/NMDAR ratio in the PFC of 12-month-old *Fmr1* KO. (*A*) Time course of TBS-LTP (TBS, indicated by arrow) in 12-month-old *Fmr1* KO mPFC slices preincubated for 1 h in 10 μM MPEP. Insert: percent LTP 35–40 min post TBS [*Fmr1* KO, $n = 13$ (period matched control subset from Fig. 1) and MPEP, $n = 11$]. (*B*) Bar chart of fEPSP percent change from baseline 35–40 min after TBS in MPEP-treated WT and *Fmr1* KO littermates. (*C*) Scatter plot of AMPAR/NMDAR ratio calculated from individual layer 5 pyramidal neurons after 1 h incubation in 10 μM MPEP. Lines represent mean and standard error (*$P < 0.05$).

FMRP regulation of synaptic mRNAs is highly promiscuous. Over a thousand different mRNA targets have thus far been identified, including a third of the postsynaptic proteasome and a quarter of the presynaptic proteasome (Darnell et al. 2011; Ascano et al. 2012). Important targets for FMRP regulation include potassium channel family members, which in the hippocampus have been linked to deficits in LTP in *Fmr1* KO mice (Lee et al. 2011). However, our recordings of the intrinsic properties from 12-month-old layer V pyramidal neurons did not identify any changes in hyperpolarization-gated currents, as reported in CA1 pyramidal neurons (Brager et al. 2012). Neither were we able to identify any changes in basic firing properties of these cells, arguing against a large change in potassium channels (Gross et al. 2011; Lee et al. 2011; Deng et al. 2013). Instead, our findings of reduced NMDAR, but not AMPAR-mediated currents, are more consistent with a direct change in synaptic glutamate receptor expression in 12-month-old *Fmr1* KO mice. Supporting this idea is the finding that in young adult *Fmr1* KO mice (2 months) NMDAR expression in synaptosomes is either normal or enhanced compared with WT mice in the neocortex (Schütt et al. 2009); however, in mice at an age intermediary to those used in this study (4 months), NMDAR expression is reduced by 15% (Krueger et al. 2011). Therefore, it is likely that the reduction in LTP found in 12-month-old *Fmr1* KO mice is directly linked to the reduction in NMDAR function.

Enhanced postsynaptic mGluR5-mediated LTD is a hallmark of FXS (Bear et al. 2004), and genetic reduction or treatment with mGluR5 antagonists rescues many of the behavioral deficits found in the *Fmr1* KO mouse (Dölen et al. 2007; Krueger and Bear 2011; Michalon et al. 2012; Busquets-Garcia et al. 2013). Furthermore, FXS individuals are reported to have enhanced expression of mGluR5 in the PFC (Lohith et al. 2013). This prompted us to ask if treatment with an mGluR5 antagonist might rescue the age-linked deficits in LTP found in the *Fmr1* KO mouse PFC. Surprisingly, we found that acute treatment with mGluR5-negative allosteric modulator MPEP for 1 h ex vivo restored TBS-LTP in 12-month-old *Fmr1* KO mice to WT levels. Furthermore, analysis of the AMPAR/NMDAR ratio in these MPEP-treated neurons suggested a normalization of NMDAR function. A similar acute treatment restored LTP in the hippocampus and anterior cingulate cortex in *Fmr1* KO mice, arguing for the validity of this approach (Gross et al. 2011; Xu et al. 2012; Chen et al. 2014). FXS shares molecular similarities to Alzheimer's disease (Sokol et al. 2011), notably an amyloid-β peptide-dependent enhancement of mGluR5 signaling and a reduction in NMDAR-mediated transmission (Renner et al. 2010; Malinow 2012; Hu et al. 2014). Similar to our findings in 12-month-old *Fmr1* KO, acute MPEP treatments are able to normalize postsynaptic mGluR5 signaling and restore NMDAR-dependent LTP in mouse models of Alzheimer's disease (Wang et al. 2004; Rammes et al. 2011; Um et al. 2013). Precisely, how mGluR5 downregulation rapidly couples to an enhancement in NMDAR function in the *Fmr1* KO PFC is unclear; however, it is worth noting that a single in vivo acute MPEP injection is able to rapidly modulate both firing properties and NMDAR function in deep layer pyramidal neurons of the PFC (Homayoun et al. 2004; Homayoun and Moghaddam 2006). Regardless, the restoration of LTP in 12-month-old *Fmr1* KO mice with mGluR5 antagonism supports the idea that aberrant mGluR activity is central to many of the synaptic dysfunctions found in FXS.

It is tempting to connect our age-linked *Fmr1* KO observations, directly to age-dependent changes in cognitive function found in FXS individuals; however, how synaptic plasticity reflects PFC-dependent behavior is currently unclear. Nonetheless, the finding that deficits in PFC function vary temporally in the *Fmr1* KO mouse extends current treatment strategies for FXS. Specifically, tailoring treatments to subject age and/or combinations of drugs might show future promise in FXS.

Authors' Contributions

H.M. and O.J.M. designed research; H.M. and O.L. performed research; H.M. and O.L. analyzed data; J.T.B. contributed analysis tools and methods; H.M. and O.J.M. wrote the paper; O.J.M. supervised the entire project.

Supplementary Material

Supplementary material can be found at: http://www.cercor.oxfordjournals.org/.

Funding

This work was supported by Institut National de la Santé et de la Recherche Médicale (INSERM); L'Agence nationale de la Recherche (ANR) Blanc France-Taiwan RescueMemo (to O.M.); ANR CYFIP-Aut; the FRAXA Research Foundation (to O.M.); NARSAD 2010 Independent Investigator Grant (to O.M.); and Foundation Jêrome Lejeune (to H.M. and O.M.).

Notes

The authors thank the FRAXA research foundation (Dr D. Nelson, Baylor College of Medicine) for providing the *Fmr1* KO2 mice. O.M. and H.M. are grateful to Dr P. Chavis, Dr Po-Wu Gean, and the Chavis and Manzoni laboratories for helpful discussion. *Conflict of Interest*: None declared.

References

Ascano M, Mukherjee N, Bandaru P, Miller JB, Nusbaum JD, Corcoran DL, Langlois C, Munschauer M, Dewell S, Hafner M, et al. 2012. FMRP targets distinct mRNA sequence elements to regulate protein expression. Nature. 492:382–386.

Bailey DB, Raspa M, Olmsted M, Holiday DB. 2008. Co-occurring conditions associated with FMR1 gene variations: findings from a national parent survey. Am J Med Genet A. 146A:2060–2069.

Bear MF, Huber KM, Warren ST. 2004. The mGluR theory of fragile X mental retardation. Trends Neurosci. 27:370–377.

Bostrom CA, Majaess N-M, Morch K, White E, Christie BR. 2013. Rescue of NMDAR-dependent synaptic plasticity in Fmr1 knock-out mice. Cereb Cortex. doi:10.1093/cercor/bht237.

Brager DH, Akhavan AR, Johnston D. 2012. Impaired dendritic expression and plasticity of h-channels in the fmr1(–/y) mouse model of Fragile X Syndrome. Cell Rep. 1:225–233.

Busquets-Garcia A, Gomis-González M, Guegan T, Agustín-Pavón C, Pastor A, Mato S, Pérez-Samartín A, Matute C, de la Torre R, Dierssen M, et al. 2013. Targeting the endocannabinoid system in the treatment of fragile X syndrome. Nat Med. 19:603–607.

Chen T, Lu J-S, Song Q, Liu M-G, Koga K, Descalzi G, Li Y-Q, Zhuo M. 2014. Pharmacological rescue of cortical synaptic and network potentiation in a mouse model for Fragile X Syndrome. Neuropsychopharmacology. 39:1955–1967.

Cornish KM, Munir F, Cross G. 2001. Differential impact of the FMR-1 full mutation on memory and attention functioning : a neuropsychological perspective. J Cogn Neurosci. 13:144–150.

Darnell JC, Van Driesche SJ, Zhang C, Hung KYS, Mele A, Fraser CE, Stone EF, Chen C, Fak JJ, Chi SW, et al. 2011. FMRP stalls ribosomal translocation on mRNAs linked to synaptic function and autism. Cell. 146:247–261.

Deng P-Y, Rotman Z, Blundon JA, Cho Y, Cui J, Cavalli V, Zakharenko SS, Klyachko VA. 2013. FMRP regulates neurotransmitter release and synaptic information transmission by modulating action potential duration via BK channels. Neuron. 77:696–711.

Dölen G, Osterweil E, Rao BSS, Smith GB, Auerbach BD, Chattarji S, Bear MF. 2007. Correction of Fragile X Syndrome in mice. Neuron. 56:955–962.

Eadie BD, Cushman J, Kannangara TS, Fanselow MS, Christie BR. 2012. NMDA receptor hypofunction in the dentate gyrus and impaired context discrimination in adult Fmr1 knockout mice. Hippocampus. 22:241–254.

Franklin AV, King MK, Palomo V, Martinez A, McMahon LL, Jope RS. 2014. Glycogen synthase kinase-3 inhibitors reverse deficits in long-term potentiation and cognition in Fragile X Mice. Biol Psychiatry. 75:198–206.

Gantois I, Pop AS, de Esch CEF, Buijsen RAM, Pooters T, Gomez-Mancilla B, Gasparini F, Oostra BA, D'Hooge R, Willemsen R. 2013. Chronic administration of AFQ056/Mavoglurant restores social behaviour in Fmr1 knockout mice. Behav Brain Res. 239:72–79.

Gocel J, Larson J. 2012. Synaptic NMDA receptor-mediated currents in anterior piriform cortex are reduced in the adult fragile X mouse. Neuroscience. 221:170–181.

Goto Y, Yang CR, Otani S. 2010. Functional and dysfunctional synaptic plasticity in prefrontal cortex: roles in psychiatric disorders. Biol Psychiatry. 67:199–207.

Gross C, Yao X, Pong DL, Jeromin A, Bassell GJ. 2011. Fragile X mental retardation protein regulates protein expression and mRNA translation of the potassium channel K_v4.2. J Neurosci. 31:5693–5698.

Harlow EG, Till SM, Russell TA, Wijetunge LS, Kind P, Contractor A. 2010. Critical period plasticity is disrupted in the barrel cortex of Fmr1 knockout mice. Neuron. 65:385–398.

Homayoun H, Moghaddam B. 2006. Bursting of prefrontal cortex neurons in awake rats is regulated by metabotropic glutamate 5 (mGlu5) receptors: rate-dependent influence and interaction with NMDA receptors. Cereb Cortex . 16:93–105.

Homayoun H, Stefani MR, Adams BW, Tamagan GD, Moghaddam B. 2004. Functional interaction between NMDA and mGlu5 receptors: effects on working memory, instrumental learning, motor behaviors, and dopamine release. Neuropsychopharmacol Off Publ Am Coll Neuropsychopharmacol. 29:1259–1269.

Hu H, Qin Y, Bochorishvili G, Zhu Y, van Aelst L, Zhu JJ. 2008. Ras signaling mechanisms underlying impaired GluR1-dependent plasticity associated with Fragile X Syndrome. J Neurosci. 28:7847–7862.

Hu N-W, Nicoll AJ, Zhang D, Mably AJ, O'Malley T, Purro SA, Terry C, Collinge J, Walsh DM, Rowan MJ. 2014. mGlu5 receptors and cellular prion protein mediate amyloid-β-facilitated synaptic long-term depression in vivo. Nat Commun. 5:doi: 10.1038/ncomms4374.

Huntley JD, Howard RJ. 2010. Working memory in early Alzheimer's disease: a neuropsychological review. Int J Geriatr Psychiatry. 25:121–132.

Iafrati J, Orejarena MJ, Lassalle O, Bouamrane L, Gonzalez-Campo C, Chavis P. 2014. Reelin, an extracellular matrix protein linked to early onset psychiatric diseases, drives postnatal development of the prefrontal cortex via GluN2B-NMDARs and the mTOR pathway. Mol Psychiatry. 19:417–426.

Kramvis I, Mansvelder H, Loos M, Meredith R. 2013. Hyperactivity, perseveration and increased responding during attentional rule acquisition in the Fragile X mouse model. Front Behav Neurosci. 7:172.

Krueger DD, Bear MF. 2011. Toward fulfilling the promise of molecular medicine in Fragile X Syndrome. Annu Rev Med. 62:411–429.

Krueger DD, Osterweil EK, Chen SP, Tye LD, Bear MF. 2011. Cognitive dysfunction and prefrontal synaptic abnormalities in a mouse model of fragile X syndrome. Proc Natl Acad Sci USA. 108:2587–2592.

Lachiewicz AM, Gullion CM, Spiridigliozzi GA, Aylsworth AS. 1987. Declining IQs of young males with the fragile X syndrome. Am J Ment Retard AJMR. 92:272–278.

Lafourcade M, Elezgarai I, Mato S, Bakiri Y, Grandes P, Manzoni OJ. 2007. Molecular components and functions of the endocannabinoid system in mouse prefrontal cortex. PLoS ONE. 2:e709.

Larson J, Jessen RE, Kim D, Fine A-KS, Du Hoffmann J. 2005. Age-dependent and selective impairment of long-term potentiation in the anterior piriform cortex of mice lacking the Fragile X mental retardation protein. J Neurosci. 25:9460–9469.

Lee HY, Ge W-P, Huang W, He Y, Wang GX, Rowson-Baldwin A, Smith SJ, Jan YN, Jan LY. 2011. Bidirectional regulation of dendritic voltage-gated potassium channels by the Fragile X mental retardation protein. Neuron. 72:630–642.

Lohith TG, Osterweil EK, Fujita M, Jenko KJ, Bear MF, Innis RB. 2013. Is metabotropic glutamate receptor 5 upregulated in prefrontal cortex in fragile X syndrome? Mol Autism. 4:15.

Malinow R. 2012. New developments on the role of NMDA receptors in Alzheimer's disease. Curr Opin Neurobiol. 22:559–563.

Martin HGS, Manzoni O. 2014. Late onset deficits in synaptic plasticity in the valproic acid rat model of autism. Front Cell Neurosci. 8:23.

Meredith RM, Holmgren CD, Weidum M, Burnashev N, Mansvelder HD. 2007. Increased threshold for spike-timing-dependent plasticity is caused by unreliable calcium signaling in mice lacking fragile X gene FMR1. Neuron. 54:627–638.

Michalon A, Sidorov M, Ballard TM, Ozmen L, Spooren W, Wettstein JG, Jaeschke G, Bear MF, Lindemann L. 2012. Chronic pharmacological mglu5 inhibition corrects Fragile X in adult mice. Neuron. 74:49–56.

Pilpel Y, Kolleker A, Berberich S, Ginger M, Frick A, Mientjes E, Oostra BA, Seeburg PH. 2009. Synaptic ionotropic glutamate receptors and plasticity are developmentally altered in the CA1 field of Fmr1 knockout mice. J Physiol. 587:787–804.

Rammes G, Hasenjäger A, Sroka-Saidi K, Deussing JM, Parsons CG. 2011. Therapeutic significance of NR2B-containing NMDA receptors and mGluR5 metabotropic glutamate receptors in mediating the synaptotoxic effects of β-amyloid oligomers on long-term potentiation (LTP) in murine hippocampal slices. Neuropharmacology. 60:982–990.

Renner M, Lacor PN, Velasco PT, Xu J, Contractor A, Klein WL, Triller A. 2010. Deleterious effects of amyloid beta oligomers acting as an extracellular scaffold for mGluR5. Neuron. 66: 739–754.

Rinaldi T, Kulangara K, Antoniello K, Markram H. 2007. Elevated NMDA receptor levels and enhanced postsynaptic long-term potentiation induced by prenatal exposure to valproic acid. Proc Natl Acad Sci USA. 104:13501–13506.

Rinaldi T, Silberberg G, Markram H. 2008. Hyperconnectivity of local neocortical microcircuitry induced by prenatal exposure to valproic acid. Cereb Cortex. 18:763–770.

Ronesi JA, Huber KM. 2008. Metabotropic glutamate receptors and fragile X mental retardation protein: partners in translational regulation at the synapse. Sci Signal. 1:pe6.

Schneider A, Ligsay A, Hagerman RJ. 2013. Fragile X syndrome: an aging perspective. Dev Disabil Res Rev. 18:68–74.

Schütt J, Falley K, Richter D, Kreienkamp H-J, Kindler S. 2009. Fragile X mental retardation protein regulates the levels of scaffold proteins and glutamate receptors in postsynaptic densities. J Biol Chem. 284:25479–25487.

Sidorov MS, Auerbach BD, Bear MF. 2013. Fragile X mental retardation protein and synaptic plasticity. Mol Brain. 6:15.

Sidorov MS, Krueger DD, Taylor M, Gisin E, Osterweil EK, Bear MF. 2014. Extinction of an instrumental response: a cognitive behavioral assay in Fmr1 knockout mice. Genes Brain Behav. 13:451–458.

Sokol DK, Maloney B, Long JM, Ray B, Lahiri DK. 2011. Autism, Alzheimer disease, and fragile X: APP, FMRP, and mGluR5 are molecular links. Neurology. 76:1344–1352.

Suvrathan A, Hoeffer CA, Wong H, Klann E, Chattarji S. 2010. Characterization and reversal of synaptic defects in the amygdala in a mouse model of fragile X syndrome. Proc Natl Acad Sci USA. 107:11591–11596.

Testa-Silva G, Loebel A, Giugliano M, de Kock CPJ, Mansvelder HD, Meredith RM. 2012. Hyperconnectivity and slow synapses during early development of medial prefrontal cortex in a mouse model for mental retardation and autism. Cereb Cortex. 22:1333–1342.

Till SM, Wijetunge LS, Seidel VG, Harlow E, Wright AK, Bagni C, Contractor A, Gillingwater TH, Kind PC. 2012. Altered maturation of the primary somatosensory cortex in a mouse model of fragile X syndrome. Hum Mol Genet. 21:2143–2156.

Um JW, Kaufman AC, Kostylev M, Heiss JK, Stagi M, Takahashi H, Kerrisk ME, Vortmeyer A, Wisniewski T, Koleske AJ, et al. 2013. Metabotropic glutamate receptor 5 is a coreceptor for Alzheimer Aβ oligomer bound to cellular prion protein. Neuron. 79:887–902.

Utari A, Adams E, Berry-Kravis E, Chavez A, Scaggs F, Ngotran L, Boyd A, Hessl D, Gane LW, Tassone F, et al. 2010. Aging in fragile X syndrome. J Neurodev Disord. 2:70–76.

Walcott EC, Higgins EA, Desai NS. 2011. Synaptic and intrinsic balancing during postnatal development in rat pups exposed to valproic acid in utero. J Neurosci. 31:13097–13109.

Wang H, Wu L-J, Kim SS, Lee FJS, Gong B, Toyoda H, Ren M, Shang Y-Z, Xu H, Liu F, et al. 2008. FMRP acts as a key messenger for dopamine modulation in the forebrain. Neuron. 59:634–647.

Wang Q, Walsh DM, Rowan MJ, Selkoe DJ, Anwyl R. 2004. Block of long-term potentiation by naturally secreted and synthetic amyloid β-peptide in hippocampal slices is mediated via activation of the kinases c-Jun N-terminal kinase, cyclin-dependent kinase 5, and p38 mitogen-activated protein kinase as well as metabotropic glutamate receptor type 5. J Neurosci. 24:3370–3378.

Wright-Talamante C, Cheema A, Riddle JE, Luckey DW, Taylor AK, Hagerman RJ. 1996. A controlled study of longitudinal IQ changes in females and males with fragile X syndrome. Am J Med Genet. 64:350–355.

Xu Z-H, Yang Q, Feng B, Liu S-B, Zhang N, Xing J-H, Li X-Q, Wu Y-M, Gao G-D, Zhao M-G. 2012. Group I mGluR antagonist rescues the deficit of D1- induced LTP in a mouse model of fragile X syndrome. Mol Neurodegener. 7:24.

Yun SH, Trommer BL. 2011. Fragile X mice: reduced long-term potentiation and N-methyl-D-aspartate receptor-mediated neurotransmission in dentate gyrus. J Neurosci Res. 89: 176–182.

Zhao M-G, Toyoda H, Ko SW, Ding H-K, Wu L-J, Zhuo M. 2005. Deficits in trace fear memory and long-term potentiation in a mouse model for fragile X syndrome. J Neurosci. 25:7385–7392.